Article

New Organoselenium (NSAIDs-Selenourea and Isoselenocyanate) Derivatives as Potential Antiproliferative Agents: Synthesis, Biological Evaluation and in Silico Calculations

Yousong Nie [1], Shaolei Li [2], Ying Lu [3], Min Zhong [3], Xiaolong Li [2], Youhong Zhang [1,*] and Xianran He [4,*]

[1] School of Environmental Ecology and Biological Engineering, Wuhan Institute of Technology, LiuFang Campus, Guanggu 1st Road, Wuhan 430205, China; yousongnie@163.com

[2] Shenzhen Fushan Biological Technology Co., Ltd., Kexing Science Park A1 1005, Nanshan Zone, Shenzhen 518057, China; lsl1917@163.com (S.L.); lixiaolong@szfs01.com (X.L.)

[3] Key Laboratory of Optoelectronic Chemical Materials and Devices of Ministry of Education, Jianghan University, Wuhan Economic and Technological Development Zone, Wuhan 430056, China; 202130773036@stu.jhun.edu.cn (Y.L.); 474488728@163.com (M.Z.)

[4] School of Medicine, Jianghan University, Wuhan Economic and Technological Development Zone, Wuhan 430056, China

[*] Correspondence: youhong@wit.edu.cn (Y.Z.); hexianran@163.com (X.H.)

Abstract: In this study, we report on the synthesis of new organoselenium derivatives, including non-steroidal anti-inflammatory drugs (NSAIDs) scaffolds and Se functionalities (isoselenocyanate and selenourea), which were evaluated against four types of cancer cell line: SW480 (human colon adenocarcinoma cells), HeLa (human cervical cancer cells), A549 (human lung carcinoma cells), MCF-7 (human breast adenocarcinoma cells). Among these compounds, most of the investigated compounds reduced the viability of different cancer cell lines. The most promising compound **6b** showed IC_{50} values under 10 μM against the four cancer cell lines, particularly to HeLa and MCF-7, with IC_{50} values of 2.3 and 2.5 μM, respectively. Furthermore, two compounds, **6b** and **6f,** were selected to investigate their ability to induce apoptosis in MCF-7 cells via modulation of the expression of anti-apoptotic Bcl-2 protein, pro-inflammatory cytokines (IL-2) and proapoptotic caspase-3 protein. The redox properties of the NSAIDs-Se derivatives were conducted by 2, 2-didiphenyl-1-picrylhydrazyl (DPPH), bleomycin-dependent DNA damage and glutathione peroxidase (GPx)-like assays. Finally, a molecular docking study revealed that an interaction with the active site of thioredoxin reductase 1 (TrxR1) predicted the antiproliferative activity of the synthesized candidates. Overall, these results could serve as a promising launch point for further designs of NSAIDs-Se derivatives as potential antiproliferative agents.

Keywords: NSAIDs; isoselenocyanate; selenourea; antiproliferative

1. Introduction

Non-steroidal anti-inflammatory drugs (NSAIDs) are a class of active pharmaceutical ingredients (API) that are widely used in the treatment of inflammatory conditions, including pain associated with arthritis, worldwide [1,2]. Since the 1980s, when the antiproliferative effect of sulindac was first observed in reducing colon adenomas [3], a growing body of studies has evaluated the chemoprevention and antiproliferative potential of NSAIDs [4–6], although their exact molecular mechanism has remained elusive.

The selenium (Se) has been recognized to play an important role in human health and disease [7,8]. In recent years, a number of studies have indicated an inverse association between Se intake and cancer risk [9–11]. There are three main categories of Se-containing compounds (inorganic, organic, and selenoproteins) with potential pharmacological properties; the most developed and studied are organoselenium compounds, which have been

shown to inhibit the initiation and postinitiation phases of chemical carcinogenesis [12]. Organic selenium compounds with diverse functional groups, including selenoesters, methylseleninic acid, isoselenocyanates, diselenides, endocyclic selenium, selenocyanates and trifluoromethyl selenides, were found to show potent antiproliferative activity [13–18] (Figure 1).
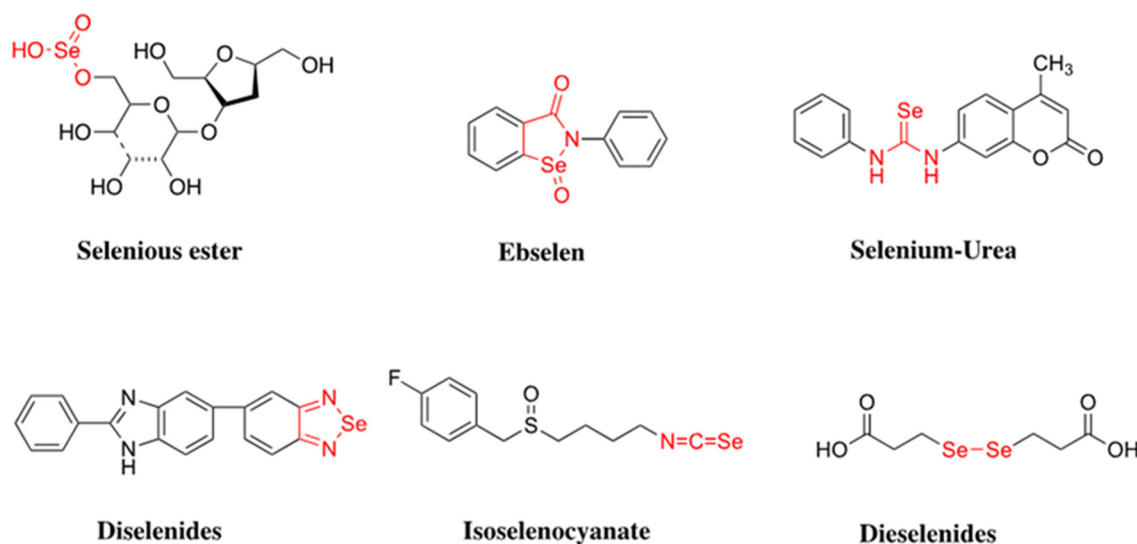
Figure 1. Organic selenium compounds with diverse fnctional groups previously reported to exhibit antiproliferative activity.

Considering the chemo-preventive effects of NSAIDs and the antiproliferative activity of organic selenium compounds, along with reports that support the modification of NSAIDs scaffolds with Se functionalities [19,20] and our continued work to search for organoselenium derivatives with antiproliferative activity [21–24], several new NSAIDs-based derivatives, combining the NSAIDs scaffold with an organoselenium motif (Isoselenocyanate and selenoureas), were synthesized in this report (Figure 2). Their antiproliferative activities against SW480, HeLa, A549 and MCF-7 cell lines were shown using the MTT (3-(4,5-dimethylthiazol-2-yl)-2,5-diphenyltetrazolium bromide) assay. Two compounds, **6b** and **6f,** were selected to test the protein expression levels of Bcl-2, IL-2 and caspase-3 biomarkers in MCF-7 cells. Furthermore, the antioxidant potential of the compounds was investigated by employing DPPH, bleomycin-dependent DNA damage and GPx-like assays. Finally, Thioredoxin Reductase (TrxR1) was selected as a docking protein to predict the target and antiproliferative activity of the prepared NSAIDs-Se hybrid compounds.
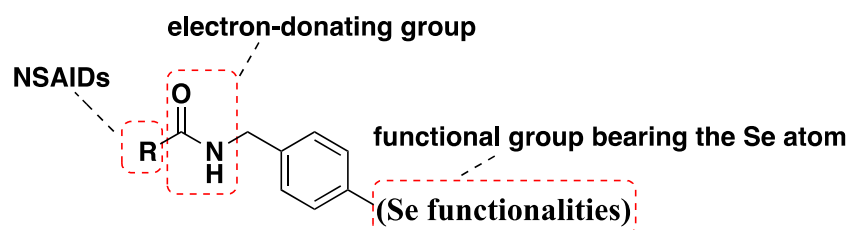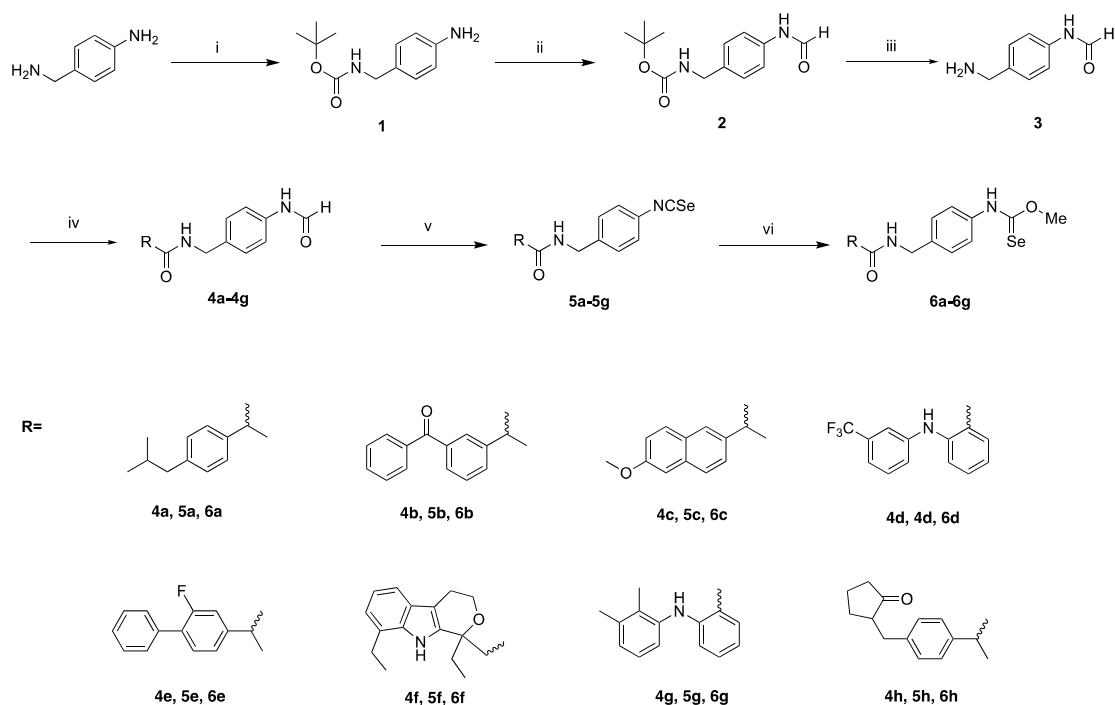

Figure 2. Structure of NSAIDs-Se derivatives.

2. Results and Discussion

2.1. Chemistry

The synthesis of novel families of NSAIDs-based seleno derivatives as potential antiproliferative agents: Isoselenocyanates (ISCs) (**5a**–**5h**) and selenoureas (**6a**–**6h**) in this study was performed as outlined in Scheme 1.

R=

Scheme 1. (i) (Boc)₂, THF, −10 °C, 2 h, 90%; (ii) HCOOH, Si(OEt)₄, CH₃CN, 85 °C, 12 h, 80%; (iii) CF₃COOH, DCM, −10 °C, 0.5 h, 90%; (iv) EDCI, HOBT, TEA, CH₂Cl₂/DMF, N₂, r.t. 0.5 h, 65–80%; (v) a, Triphosgene, TEA, DCM, N₂, reflux, 2 h. b, Se, N₂, reflux, 12 h; (vi) MeOH, reflux, 4 h, 90%.

The synthesis of the NSAIDs-Isoselenocyanate derivatives (**5a–5h**) (Purity ≥ 95% by HPLC) was started from 4-aminobenzylamine protected by bis(1,1-dimethylethyl) ester to afford compound **1**. Compound **1** was transformed into formamide **2** upon treatment with formic acid, with 80% yield. Next, compound **3** was obtained by deprotecting Boc-group in trifluoroacetic acid (TFA) and Dichloromethane (DCM) system. Compounds **4a–4h** (Purity ≥ 95% by HPLC, except 4g) were obtained by commercially available NSAIDs and compound **3** in the presence of EDCI and HOBT as condensantion agent, in DMF as sovent and under a nitrogen atmosphere. Then, compounds **4a–4h** were transformed into the NSAIDs-based isoselenocyanate (**5a–5h**) (Scheme 1) in a one-pot two-step procedure, which involves triphosgene-based dehydration of **4a–4h** into a transient non-isolated isocyanide, followed by the addition of elemental selenium black (70% overall yield).

NSAIDs-selenourea derivatives (**6a–6h**) (Purity ≥ 95% by HPLC) were obtained by conducting corresponding NSAIDs-Isoselenocyanate derivatives with methanol.

2.2. Cell Viability Assay

MTT assay was conducted to evaluate the potential antiproliferative activities against human tumor cell lines derived from various human cancer types: SW480 (human colon adenocarcinoma cells), HeLa (human cervical cancer cells), A549 (human lung carcinoma cells), MCF-7 (human breast adenocarcinoma cells) of target compounds **5a–5h** and **6a–6h**, 5-Fu was selected as reference standard (Table 1).

Overall, the IC₅₀ values obtained and summarized in Table 1 show that allfthe tested organoselenium compounds with NSAIDs scaffolds and Se functionalities (isoseleno-cyanate and selenourea) exhibit growth inhibition in all cancer cell lines, while the selected patent NSAIDs (Aspirin, Ibuprofen and Naproxen) are inactive against all cells, even at the maximum dose of 50 μM.

An overview analysis of the IC₅₀ values obtained and summarized in Table 1 showed that most of the NSAIDs-selenourea derivatives wer emore effective than NSAIDs-isoseleno-cyanate derivatives against all four cancer cell lines. Furthermore, the most active com-

pounds of these two series were **6b** and **6f**. These two compounds show IC_{50} values below 10 μM in all tested cancer cell lines. Compound **6b** was the most potent agent, with IC_{50} values below 5 μM in all cancer cell lines and remarkable antiproliferative activity against HeLa (2.3 μM) and MCF-7 (2.5 μM).

Table 1. Antiproliferative Activity of Target Compounds against four Human Cancer Cell Lines.

Compound	IC_{50} (μM) [a]			
	SW480	HeLa	A549	MCF-7
Aspirin [b]	>50	>50	>50	>50
Ibuprofen [b]	>50	>50	>50	>50
Naproxen [b]	>50	>50	>50	>50
5a	24.3 ± 1.8	20.4 ± 2.1	16.4 ± 1.0	27.3 ± 1.7
5b	16.5 ± 1.2	32.5 ± 2.4	21.4 ± 1.4	24.5 ± 2.3
5c	29.4 ± 2.1	32.6 ± 3.1	26.3 ± 1.7	19.8 ± 1.4
5d	18.2 ± 1.3	27.1 ± 1.5	27.3 ± 2.2	30.2 ± 3.1
5e	13.3 ± 1.2	18.3 ± 1.4	24.3 ± 2.2	28.4 ± 2.5
5f	31.4 ± 2.8	19.3 ± 1.7	30.8 ± 2.7	24.4 ± 1.8
5g	13.4 ± 0.8	9.7 ± 1.2	14.2 ± 1.5	7.5 ± 1.2
5h	26.6 ± 2.2	19.7 ± 1.4	35.7 ± 3.0	24.3 ± 1.9
5i	31.6 ± 2.6	12.6 ± 1.6	8.8 ± 0.7	9.6 ± 0.7
5j	17.3 ± 1.3	15.4 ± 1.3	9.2 ± 0.5	12.2 ± 1.3
5h	30.4 ± 2.8	20.2 ± 1.7	10.4 ± 0.8	15.4 ± 1.4
6a	24.4 ± 1.6	32.4 ± 2.8	19.7 ± 1.2	9.3 ± 0.5
6b	8.5 ± 0.6	2.3 ± 0.3	4.9 ± 0.7	2.5 ± 0.5
6c	27.5 ± 1.9	19.3 ± 1.2	21.6 ± 1.8	11.8 ± 1.3
6d	13.3 ± 1.6	19.6 ± 2.1	8.5 ± 1.3	24.3 ± 2.3
6e	11.4 ± 1.2	16.5 ± 1.4	18.7 ± 0.9	21.7 ± 1.8
6f	9.3 ± 0.4	7.6 ± 0.4	6.2 ± 0.4	6.4 ± 0.5
6g	11.5 ± 1.2	8.7 ± 0.3	12.4 ± 1.7	9.8 ± 0.7
6h	16.4 ± 2.2	14.5 ± 1.3	21.3 ± 2.4	14.6 ± 0.9
6i	19.9 ± 1.2	8.8 ± 0.3	8.5 ± 0.6	8.4 ± 1.1
6j	11.3 ± 1.5	13.2 ± 0.7	7.7 ± 0.8	10.3 ± 0.7
6h	21.4 ± 2.0	17.2 ± 1.5	9.9 ± 0.6	12.4 ± 1.3
5-Fu [c]	12.3 ± 1.3	9.4 ± 1.3	15.4 ± 2.1	7.5 ± 0.9

[a] IC_{50} values (±SD) of % cell viability determined by the MTT assay of three repititions; [b] Patent NSAIDs; [c] Standard benchmark compound.

2.3. Evaluation of Bcl-2, IL-2 and Caspase-3 Molecular Biomarkers in MCF-7 Cells

To further understand the possible mechanism of the reduced cell viability of the target compounds, **6b** and **6f** were selected for their ability to induce apoptosis in MCF-7 cells via modulation of the expression of some apoptosis-related proteins (e.g., Bcl-2, IL-2, caspase-3). Protein levels of the anti-apoptotic marker Bcl-2 were measured using enzyme-linked immunosorbent assay (ELISA) according to the manufacturers' instructions (Merck, Rahway, NJ, USA). Enzyme-linked immunosorbent assay was used for the quantitative detection of IL-2 and caspase-3 (Platinum ELISA).

As shown in Table 2, **6b** and **6f** were able to downregulate the expression of Bcl-2 and upregulate the expression of IL-2 and Caspase-3 in MCF-7 cells compared with untreated cells. Compound **6f** downregulated over 50% of the expression levels of Bcl-2 compared to untreated cells. Furthermore, compound **6b** modulated the IL-2 level to a 1.5-fold increase in expression when compared to the untreated control cells. Finally, compound **6b** exhibited a superior activity increased the expression level of caspase-3 by 5-fold compared to untreated cells. From these results, it is likely that compounds **6b** and **6f** may induce apoptosis to inhibit tumor cells growth, in line with the underlying mechanism of some organoselenium compounds, which were reported to be effective against prostate and oral carcinoma cells via the estimation of potential biomarkers [15].

Table 2. Protein expression levels of Bcl-2, IL-2 and caspase-3 in MCF-7 cells after 48 h incubation with compounds **6b** and **6f** at their respective IC_{50}s compared to untreated cells.

Compound	Protein Expression Levels		
	Bcl-2	**Caspase-3**	**IL-2**
Vehicle	57	1.95	70
6b	44	10.88	150
6f	28	8.01	112

2.4. Antioxidant Assay

Reactive oxygen species (ROS), e.g., H_2O_2, $O_2{}^-$, $HO^{\cdot}$, and $HOCl$, serve important physiological roles that include signaling functions, host defense, and oxidative biosynthesis [25].

Various human diseases, including different types of cancer, are associated with a disturbed intracellular redox balance and oxidative stress (OS) [26]. Redox modulators play an important role as chemotherapeutic potential antitumor agents [27].

As a number of synthetic organoselenium compounds have been synthesized for their use as redox-modulators in recent years [28,29], the antioxidant activity of the selected synthesized compounds are further estimated by employing different biochemical assays such as DPPH, bleomycin-dependent DNA damage and Gpx-like assays [30–32].

2.4.1. Radical Scavenging Capacity (DPPH) Assay

The DPPH scavenging capacity assay is considered a valid and rapid colorimetric method for antioxidant property evaluation. This assay has been successfully utilized for investigating the antioxidant properties of nutritional products and organic selenides [33,34].

As depicted in Table 3, NSAIDs-selenourea derivatives **6b**, **6f** and **6h** were the most active compounds in this assay, demonstrating a good free-radical scavenging activity compared to Vitamin C. The family of NSAIDs-selenourea derivatives is better than the corresponding NSAIDs-isoselenocyanate derivatives on this assay, except when comparing **5d** and **6d**.

Table 3. Redox modulation activity of NSAID-Se hybrid compounds.

Compd. No.	DPPH Assay		Bleomycin-Dependent DNA Damage Assay
	Inhibition %	**Fold**	**Absorbance**
Vitamin C	91.5 ± 1.8	1	287 ± 2.95
5a	17.2 ± 1.3	0.2	78.6 ± 0.63
5b	21.3 ± 1.5	0.2	65.4 ± 0.54
5c	22.5 ± 1.4	0.2	72.8 ± 0.44
5d	51.3 ± 2.7	0.5	99.6 ± 1.84
5e	29.4 ± 1.3	0.3	74.7 ± 0.55
5f	17.6 ± 1.1	0.2	82.4 ± 0.78
5g	22.0 ± 1.3	0.2	94.2 ± 0.73
5h	40.3 ± 2.3	0.4	101.4 ± 1.29
6a	30.4 ± 2.0	0.3	87.5 ± 0.62
6b	60.5 ± 3.5	0.6	97.5 ± 1.23
6c	42.6 ± 2.4	0.4	88.3 ± 1.48
6d	28.5 ± 1.6	0.3	94.3 ± 1.55
6e	44.4 ± 2.7	0.4	80.4 ± 1.40
6f	68.2 ± 3.0	0.7	91.6 ± 1.24
6g	28.6 ± 1.7	0.3	102.7 ± 2.24
6h	60.3 ± 2.8	0.6	87.6 ± 1.23

2.4.2. Bleomycin DNA Damage Assay

Bleomycin (BLM) is a family of glycopeptide antibiotics that are routinely used as antitumor agents; it is believed to oxidize DNA and induces single- and double-strand

breaks [35,36]. The bleomycin-iron DNA damage assay has routinely been used as a preliminary method to test the potential of drugs and organic selenium compounds [37]. As shown in Table 3, compounds **5d**, **5h** and **6g** induced DNA degradation significantly more than other tested compounds.

2.4.3. Glutathione Peroxidase-like Activity Assay

Glutathione peroxidase (GPx) is a well-known selenoenzyme that functions as an antioxidant [38,39]. The potential antioxidant activity of all the NSAIDs-Se derivatives were estimated using an NADPH-reductase coupled assay [40,41]. The GPx activity of the synthesized compounds was estimated by the decrease in absorbance (340 nm) due to the oxidation of NADPH to NADP$^+$. Ebselen was used as a positive control.

As shown in Table 4, compounds **6a–6h** displayed a better GPx-like activity than the respective **5a–5h** derivatives. Compound **6g** was the most active derivative in this assay, reaching up to 1.5-fold of the GPx mimetic ebselen.

Table 4. GPx-like activity assay of NSAID-Se hybrid compounds in μM. Min^{-1}.

Compound	GPx-like Activity Assay
	Rate (μM·min^{-1})
Ebselen	0.008
5a	0.005
5b	0.0062
5c	0.0068
5d	0.0071
5e	0.0068
5f	0.0077
5g	0.0063
5h	0.0051
6a	0.011
6b	0.013
6c	0.012
6d	0.0088
6e	0.0085
6f	0.01
6g	0.014
6h	0.009

2.5. Docking Studies

TrxR1 consists of four monimers, which have FAD and NAD binding domains at the N-terminal and the dimerization interface domain at the flexible C-terminal side. The binding mode between organoselenium compounds and Mammalian TrxR1 protein was described by docking studies. TrxR1 consists of several functional domains, including FAD- and NAD-binding domains at the N-terminal, and the dimerization interface domain at the flexible C-terminal side [42–44]. It has been reported that flexible docking can simulate the interaction between small molecules and TrxR1 [45]. Therefore, compounds **6b** and **6f** were docked into the TrxR1 protein (PDB id: 1H6V) using the Flexible Docking Protocol, as reported in the literature [45]. The distances between the selenium atom of all two compounds and Cys497/Cys498 of TrxR1 were measured and focused on because they are closely related to the accessibility of cysteine thiol attack selenides.

The pose 2 of compound **6b** showed high -CDOCKER energy values (21.223 kcal/mol) and a close distance between the selenium atom and Cys498 (7.489 Å). Multiple interactions were found in this conformation, including electrostatic (Pi-Anion) between the benzene and GLU477 (4.326 Å), hydrogen bonding between the hydrogen of secondary amine of Seleno-carbamates and GLU477 (2.097 Å), and hydrogen bonding between the hydrogen of hydroxyl of Seleno-carbamates and GLU477 (2.549 Å) (Table 5, Pose 2; Figure 3). Compound **6f** had multiple interactions with GLY496, which was adjacent to the key amino acid

Cys497/Cys498. In pose 1, the value of -CDOCKER energy was 33.662 kcal/mol and distance between the selenium atom and Cys498 was 5.167 Å (Table 6, Pose 1). Three hydrogen bondings appear in this conformation, including the hydrogen bonding between the nitrogen of selenocarbamates and GLU477 (2.834 Å), the hydrogen bonding between the hydrogen of amide bond and GLY496 (2.776 Å) and the hydrogen bonding between the oxygen of amide bond and GLY496 (2.494 Å) (Figure 4).

Table 5. Ligand-protein poses for compound **6b**.

Pose Index	-CDOCKER_ENERGY	-CDOCKER_INTERRATION _ENERGY	Distance Cys497Se	Distance Cys498Se
1	26.7498	38.7932	13.309	11.180
2	25.9117	37.1133	11.189	7.489
3	24.7841	37.3573	12.661	9.895
4	24.4515	36.8086	13.352	11.245
5	23.9085	36.3628	13.360	11.270
6	23.2581	35.6687	13.004	10.744
7	23.2402	35.5194	13.424	11.342
8	22.888	34.7432	10.364	11.288
9	22.8783	35.474	15.857	9.295
10	22.7819	34.0384	11.241	9.814
11	21.8846	35.9701	12.512	10.023
12	21.8833	34.1865	11.286	8.155
13	20.9353	33.4574	12.187	10.603
14	20.9345	33.2165	15.031	8.258
15	20.5401	32.9407	12.311	10.654
16	20.0725	32.6116	15.034	6.869
17	20.0267	32.588	14.556	7.882
18	19.9849	36.4132	15.780	14.165
19	19.8432	32.9191	13.107	10.920
20	19.7226	30.3231	10.969	7.250
21	19.5466	34.0942	13.325	11.205
22	19.5319	34.3359	14.603	13.686
23	19.4702	30.0589	10.964	5.421
24	19.166	31.5076	12.256	9.907
25	19.0302	34.1211	15.695	14.076
26	18.9631	33.1387	13.075	10.797
27	18.8205	33.4487	14.428	13.446
28	18.7366	32.7512	13.253	11.014
29	18.4295	33.7184	13.295	11.188
30	18.3109	32.5716	12.272	10.744

Table 6. Ligand-protein poses for compound **6f**.

Pose Index	-CDOCKER_ENERGY	-CDOCKER_INTERRATION _ENERGY	Distance Cys497Se	Distance Cys498Se
1	33.6616	41.3973	11.712	5.167
2	33.6457	41.2952	12.744	6.590
3	33.291	40.9393	13.088	8.328
4	33.2132	41.1079	12.913	6.682
5	33.1387	40.3404	12.501	6.358
6	31.9766	41.0476	12.968	7.063
7	31.6378	40.634	12.750	10.394
8	31.4432	38.4133	11.476	4.274

Table 6. *Cont.*

Pose Index	-CDOCKER_ENERGY	-CDOCKER_INTERRATION _ENERGY	Distance Cys497Se	Distance Cys498Se
9	29.5153	36.1452	13.351	11.311
10	29.2182	38.8037	13.339	8.316
11	29.1943	36.9631	13.361	11.327
12	28.8669	37.3377	11.982	5.747
13	28.0394	37.8138	15.914	14.320
14	27.88	37.6957	15.932	14.339
15	27.5992	39.9785	12.622	10.630
16	27.4292	34.7973	12.462	7.700
17	27.2011	37.7382	13.024	10.879
18	27.1549	36.954	12.233	10.787
19	26.3713	36.2804	12.058	5.521
20	26.2274	37.3707	12.736	10.403
21	26.0031	36.2979	14.981	13.686
22	25.8325	37.6781	14.471	13.512
23	25.6065	36.9761	13.394	11.342
24	25.3846	35.7122	15.463	14.029
25	25.1377	36.0201	15.712	14.094
26	24.6081	34.284	10.748	6.542
27	24.4729	36.2445	15.743	14.126
28	23.8165	35.693	14.575	13.631
29	23.4664	36.1819	15.040	13.836
30	23.2005	34.206	14.575	13.673
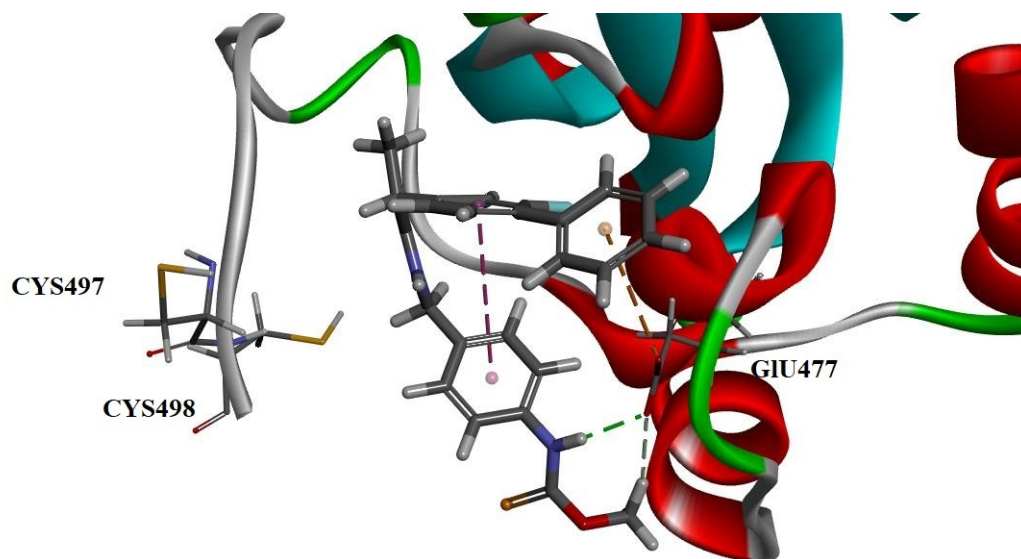
Figure 3. The pose 2 of **6b**. Three interactions were shown: electrostatic (Pi–Anion) between the benzene and GLU477 (4.326 Å), hydrogen bonding between the hydrogen of secondary amine of Seleno-carbamates and GLU477 (2.097 Å), and hydrogen bonding between the hydrogen of hydroxyl of Seleno-carbamates and GLU477 (2.549 Å).
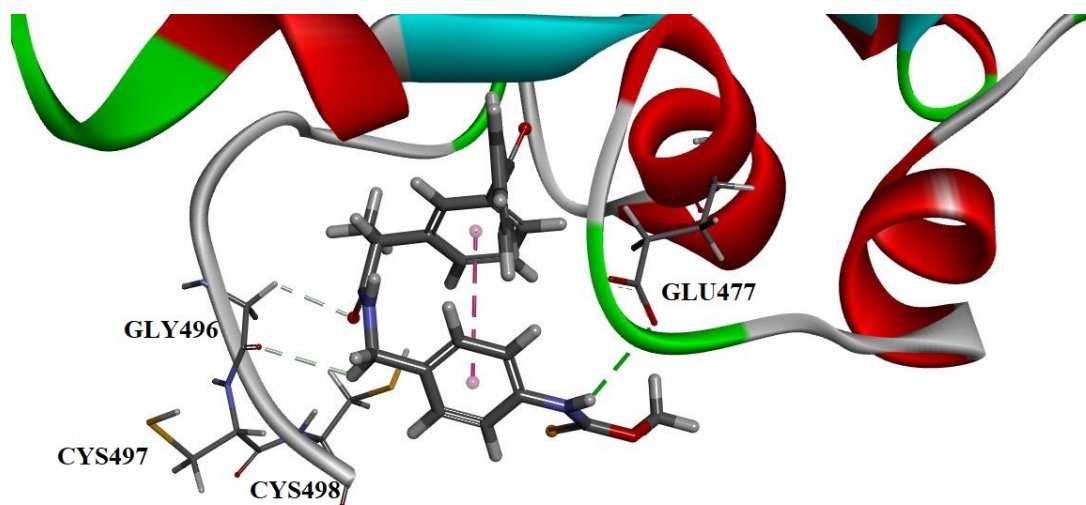
Figure 4. The pose 1 of **6f**. Three interactions are shown: hydrogen bonding between the fluorine of -SeCF$_3$ group and Ser404 (2.80 Å); hydrogen bonding between the two hydrogens on carbonyl group α position and Ile492 (2.54 Å, 2.64 Å) or Gln494 (2.90 Å); hydrogen bonding between the oxygens of ester groups and Phe406 (2.46 Å).

3. Conclusions

In conclusion, the present study involved the synthesis of new organoselenium derivatives, including NSAIDs scaffolds and Se functionalities (isoselenocyanate and selenourea). Compound **6b** exhibited the most potent activity in the MTT assay, with remarkable antiproliferative activity against HeLa (IC$_{50}$ = 2.3 μM) and MCF-7 (IC$_{50}$ = 2.5 μM). Compounds **6b** and **6f** were selected to verify if organic selenides can induce apoptosis in MCF-7 cells by modulating the expression of the Bcl-2, IL-2 and caspase-3 molecular biomarkers. The selected compounds were able to downregulate the expression of Bcl-2 and upregulate the expression of IL-2 and Caspase-3 in MCF-7 cells compared with untreated cells. Furthermore, most of the synthesized NSAIDs-Se hybrid compounds exhibited antioxidant activity in antioxidant evaluation, including DPPH, bleomycin-dependent DNA damage and Gpx-like assays.

Finally, in a flexible docking study performed on the TrxR1 enzyme, compound **6b** showed promising binding energies and a promising binding mode for the distance between the selenium atom and Cys497/Cys498. At this point, compound **6b** may act as a TrxR inhibitor. Further investigations of antiproliferative candidates based on these results are in progress.

4. Materials and Methods

4.1. Materials

All chemical reagents for the synthesis of the compounds were purchased from Macklin (Shanghai, China) or TCI (Shanghai, China) and used without further purification unless stated otherwise. TLCs were performed on aluminium pre-coated sheets (E. Merck Silica gel 60 F254). Melting points (uncorrected) were recorded on an Electrothermal apparatus. ^{1}H (400 MHz), ^{13}C (100 MHz) NMR and ^{19}F (376 MHz) spectra were recorded at 25 °C on a Bruker Avance 400 MHz spectrometer with 5-mm PABBO probe. Chemical shifts (δ) are reported in parts per million (ppm) and the coupling constants (*J*) are expressed in Hertz (Hz). Mass analysis was recorded on an ESI source mass detector (Thermo LCQ FLEET).

4.2. Experimental Procedures

4.2.1. N-(4-(aminomethyl)phenyl)formamide 3

Trifluoroacetic acid (TFA, 1.2 eq.) was added to a solution of compound **2** (1.0 eq.) in DCM (5 mL) at −10 °C. The mixture was stirred at −10 °C for 1 h. TLC showed the

reaction was complete. The mixture was concentrated under reduced pressure. The crude was diluted with DCM (10 mL) and the PH was adjusted to 8~9 by TEA. The mixture was used in the next step without purification.

4.2.2. General Procedure for the Synthesis of Compounds **4a–4h**

1-ethyl-3(3-dimethylpropylamine) carbodiimide (EDCI, 1.2 eq.), 1-hydroxybenzotriazole (HOBT, 1.2 eq.) and TEA (3.0 eq.) was added to a solution of patent NSAIDS (1.o eq.) in DCM (5 mL) and DMF (5 mL). The mixture was stirred at 25 °C for 30 min under nitrogen atmosphere. Then, N-(4-(aminomethyl)phenyl)formamide (compound **3**, 1.2 eq.) was added to the mixture. The mixture was stirred at 25 °C for 16 h under inert atmosphere. TLC showed the reaction was complete. The mixture was diluted with H_2O (20 mL); the aqueous layer was extracted with DCM (15 mL × 2); the combined organic layer was washed with brine (20 mL × 3), dried over Na_2SO_4 and filtered, and the filtrate was concentrated under reduced pressure. The residue was purified by column chromatography on silica gel, eluting with dichloromethane/methanol solution to obtain the desired compound.

N-(4-formamidobenzyl)-2-(4-isobutylphenyl)propenamide (**4a**)

Yield: 68%. White solid. Mp: 87–89 °C. ^{1}H NMR (400 MHz, CDCl₃): δ 0.86 (d, *J* = 8.00 Hz, 6H, 2 × -CH₃), 1.34 (d, *J* = 8.00 Hz, 3H, -CH₃), 1.77–1.84 (m, 1H, -CH), 2.41 (d, *J* = 8.00 Hz, 2H, -CH₂), 3.63 (q, *J* = 8.00 Hz, 1H, -CH), 4.18–4.20 (m, 2H, -CH₂), 7.06–7.09 (m, 4H, Ar-H), 7.23–7.25 (m, 2H, Ar-H), 7.46–7.48 (m, 2H, Ar-H), 8.24 (s, 1H, -NH), 8.41–8.44 (m, 1H, -NH), 10.16 (s, 1H, -CHO). ^{13}C NMR (100 MHz, CDCl₃): δ 18.9, 22.6, 30.1, 42.0, 44.7, 45.2, 117.9, 119.4, 127.5, 128.0, 128.6, 129.2, 135.2, 137.3, 139.7, 140.0, 159.9, 162.9, 173.9. MS(ESI): m/z = found 339.5 ([M + H]⁺).

2-(3-benzoylphenyl)-*N*-(4-formamidobenzyl)propenamide (**4b**)

Yield: 75%. White solid. Mp: 95–97 °C. ^{1}H NMR (400 MHz, CDCl₃): δ 1.40 (d, *J* = 8.00 Hz, 3H, -CH₃), 3.80 (q, *J* = 8.00 Hz, 1H, -CH), 4.19–4.22 (m, 2H, -CH₂), 7.08–7.10 (m, 2H, Ar-H), 7.48–7.77 (m, 11H, Ar-H), 8.24 (s, 1H, -NH), 8.55–8.58 (m, 1H, -NH), 10.17 (s, 1H, -CHO). ^{13}C NMR (100 MHz, CDCl₃): δ 18.9, 42.1, 45.4, 117.9, 119.5, 128.0, 128.6, 129.0, 130.1, 132.1, 133.2, 135.0, 137.4, 137.5, 143.2, 159.9, 162.9, 173.3, 196.3. MS(ESI): m/z = found 387.5 ([M + H]⁺).

N-(4-formamidobenzyl)-2-(6-methoxynaphthalen-2-yl)propenamide (**4c**)

Yield: 70%. White solid. Mp: 82–84 °C. ^{1}H NMR (400 MHz, DMSO): δ1.44 (d, *J* = 8.00 Hz, 3H, -CH₃), 3.79 (q, *J* = 8.00 Hz, 1H, -CH), 3.87 (s, 3H, -OCH₃), 4.19–4.21 (m, 2H, -CH₂), 7.07–7.16 (m, 4H, Ar-H), 7.29 (s, 1H, Ar-H), 7.46–7.49 (d, 1H, *J* = 8.00 Hz, Ar-H), 7.73–7.79 (m, 3H, Ar-H), 8.24 (s, 1H, -NH), 8.50 (s, 1H, -NH), 10.1 (s, 1H, -CHO). ^{13}C NMR (100 MHz, DMSO): δ 19.0, 42.2, 45.5, 55.6, 106.1, 117.9, 119.1, 119.5, 125.8, 126.7, 128.1, 128.7, 129.6, 133.6, 135.2, 137.3, 137.9, 157.5, 159.9, 163.0, 173.8. MS(ESI): m/z = found 363.4 ([M + H]⁺).

N-(4-formamidobenzyl)-2-((3-(trifluoromethyl)phenyl)amino)benzamide (**4d**)

Yield: 75%. White solid. Mp: 77–79 °C. ^{1}H NMR (400 MHz, DMSO): δ 4.34–4.42 (m, 2H, -CH₂), 6.95–6.99 (m, 1H, Ar-H), 7.13–7.28 (m, 4H, Ar-H), 7.35–7.43 (m, 4H, Ar-H), 7.45–7.47 (m, 1H, Ar-H), 7.52–7.58 (m, 2H, Ar-H), 7.73 (brs, 1H, -NH), 8.25 (brs, 1H, -NH), 9.12 (brs, 1H, -NH), 9.69 (s, 1H, -CHO). ^{13}C NMR (100 MHz, DMSO): δ 42.6, 114.6, 117.3, 117.5, 118.0, 119.6, 119.7, 120.4, 121.6, 122.1, 123.3, 126.0, 127.3 (q, *J* = 271 Hz), 128.3, 128.6, 128.9, 129.5, 130.6 (q, *J* = 32 Hz), 130.9, 132.4, 135.0, 137.4, 143.0, 143.6. MS(ESI): m/z = found 414.4 ([M + H]⁺).

2-(2-fluoro-[1,1'-biphenyl]-4-yl)-*N*-(4-formamidobenzyl)propenamide (**4e**)

Yield: 70%. White solid. Mp: 82–84 °C. ^{1}H NMR (400 MHz, DMSO): δ1.40 (d, *J* = 8.00 Hz, 3H, -CH₃), 3.74 (q, *J* = 8.00 Hz, 1H, -CH), 4.23 (s, 2H, -CH₂), 7.14–7.16 (m, 2H, Ar-H), 7.25–7.27 (m, 2H, Ar-H), 7.39–7.41 (m, 1H, Ar-H), 7.46–7.55 (m, 7H, Ar-H), 8.25 (s,

1H, -NH), 8.54 (s, 1H, -NH), 10.15 (s, 1H, -CHO). ^{13}C NMR (100 MHz, DMSO): δ 18.8, 42.3, 45.1, 115.3 (d, *J* = 92 Hz), 118.0, 119.5, 124.3, 126.8 (d, *J* = 28 Hz), 128.2, 128.7, 129.1, 129.2, 131.0, 135.1, 135.5, 137.4, 144.6, 158.1, 160.0, 160.5, 163.0, 173.2. MS(ESI): m/z = found 377.4 ([M + H]$^+$).

2-(1,8-diethyl-1,3,4,9-tetrahydropyrano[3,4-b]indol-1-yl)-*N*-(4-formamidobenzyl) acetamide (**4f**)

Yield: 72%. White solid. Mp: 102–104 °C. ^{1}H NMR (400 MHz, DMSO): δ 0.66 (t, *J* = 4.00 Hz, 3H, -CH$_3$), 1.26 (t, *J* = 4.00 Hz, -CH$_3$), 2.02–2.08 (m, 2H, -CH$_2$), 2.57–2.70 (m, 2H, CH$_2$), 2.72–2.76 (m, 1H, -CH), 2.81.2.87 (m, 2H, -CH$_2$), 2.89–2.93 (m, 1H, -CH), 3.96–3.98 (m, 2H, -CH$_2$), 4.17–4.32 (m, 2H, -CH$_2$), 6.88–6.91 (m, 2H, Ar-H), 7.04–7.16 (m, 2H, Ar-H), 7.23–7.25 (m, 1H, Ar-H), 7.48–7.50 (m, 1H, Ar-H), 8.13–8.15 (m, 1H, -NH), 10.16 (s, 1H, -NH), 10.54 (s, 1H, -CHO). ^{13}C NMR (100 MHz, DMSO): δ 8.3, 14.8, 22.4, 24.2, 31.0, 42.1, 44.4, 60.4, 76.0, 107.4, 115.9, 117.9, 119.2, 119.5, 120.1, 126.6, 127.0, 128.0, 128.5, 134.9, 137.2, 159.9, 162.9, 169.8. MS(ESI): m/z = found 420.5 ([M + H]$^+$).

2-((2,3-dimethylphenyl)amino)-*N*-(4-formamidobenzyl)benzamide (**4g**)

Yield: 65%. White solid. Mp: 109–110 °C. ^{1}H NMR (400 MHz, DMSO): δ 2.10 (s, 3H, -CH$_3$), 2.27 (s, 3H, -CH$_3$), 4.44–4.45 (m, 2H, -CH$_2$), 6.73–6.76 (m, 1H, Ar-H), 6.83–6.86 (m, 1H, Ar-H), 6.92–6.94 (m, 1H, Ar-H), 7.04–7.08 (m, 2H, Ar-H), 7.15–7.27 (m, 2H, Ar-H), 7.29–7.32 (m, 2H, Ar-H), 7.55–7.57 (m, 1H, Ar-H), 7.72–7.74 (m, 1H, Ar-H), 8.26 (s, 1H, -NH), 9.10 (s, 1H, -NH), 9.61(s, 1H, -NH), 10.2 (s, 1H, -CHO). ^{13}C NMR (100 MHz, DMSO): δ 14.0, 20.7, 42.5, 114.3, 117.2, 118.1, 119.6, 120.4, 125.6, 126.3, 128.3, 128.8, 129.1, 130.0, 132.5, 135.2, 137.4, 138.2, 139.7, 146.8, 159.9, 163.0, 169.5. MS(ESI): m/z = found 374.5 ([M + H]$^+$).

N-(4-formamidobenzyl)-2-(4-((2-oxocyclopentyl)methyl)phenyl)propenamide (**4h**)

Yield: 68%. White solid. Mp: 107–109 °C. ^{1}H NMR (400 MHz, CDCl$_3$): δ 1.34 (d, *J* = 8.00 HZ, 3H, -CH$_3$), 1.45–1.50(m, 1H, -CH-), 1.65–1.72 (m, 1H, -CH-), 1.83–1.95 (m, 2H, -CH$_2$), 1.99–2.11 (m, 1H, -CH-), 2.21–2.28 (m, 1H, -CH-), 2.35–2.46 (m, 2H, -CH$_2$), 2.93–2.97 (m, 1H, -CH-), 3.62 (q, *J* = 8.00 Hz, -CH), 4.18–4.20 (m, 2H, -CH$_2$), 7.07–7.11 (m, 4H, Ar-H), 7.23–7.25 (m, 2H, Ar-H), 7.47–7,49 (m, 2H, Ar-H), 8.24 (s, 1H, -NH), 8.41–8.44 (m, 1H, -NH), 10.16 (s, 1H, -CHO). ^{13}C NMR (100 MHz, CDCl$_3$): δ 18.9, 20.5, 29.2, 35.0, 38.1, 42.1, 45.2, 50.5, 117.9, 119.4, 127.7, 128.0, 128.6, 129.0, 135.2, 135.4, 137.4, 138.7, 140.3, 159.9, 162.9, 173.8, 220.3. MS(ESI): m/z = found 379.5 ([M + H]$^+$).

4.2.3. General Procedure for the Synthesis of Compounds **5a**–**5h**

A solution of triphosgene (0.5 eq.) in CH$_2$Cl$_2$ (5 mL) was slowly added to a solution of compound **4** (**a**–**h**) (1.0 eq.), Et$_3$N (4.0 equiv) and CH$_2$Cl$_2$ (5 mL). The resulting mixture was refluxed for 2.0 h in the dark and under a nitrogen atmosphere. Then, selenium (2.0 eq.) was added, and the mixture was refluxed for a further 12 h. TLC showed the reaction was complete. The desired compound was purified by column chromatogragraphy on silica gel.

2-(4-isobutylphenyl)-*N*-(4-isoselenocyanatobenzyl)propenamide (**5a**)

Yield: 80%. White solid. Mp: 82–84 °C. ^{1}H NMR (400 MHz, DMSO): δ 0.86 (d, 6H, *J* = 8.00 Hz, 2CH$_3$), 1.35 (d, 3H, *J* = 8.00 Hz, -CH$_3$), 1.79 (q, 1H, *J* = 8.00 Hz, -CH), 2.41 (d, 2H, *J* = 8.00 Hz, -CH$_2$), 3.64 (q, 1H, *J* = 8.00 Hz, -CH), 4.21–4.23 (m, 2H, -CH$_2$), 7.08–7.10 (m, 4H, Ar-H), 7.24–7.28 (m, 4H, Ar-H), 10.06 (s, 1H, -NH). ^{13}C NMR (100 MHz, DMSO): δ 19.0, 22.7, 30.1, 42.0, 44.7, 45.3, 125.0, 126.6, 127.5, 129.3, 136.9, 138.7, 139.8, 140.0, 173.9. MS(ESI): m/z = found 401.0 ([M + H]$^+$).

2-(3-benzoylphenyl)-*N*-(4-isoselenocyanatobenzyl)propenamide (**5b**)

Yield: 78%. White solid. Mp: 88–90 °C. ^{1}H NMR (400 MHz, DMSO): δ 1.41 (d, 3H, *J* = 8.00 Hz, -CH$_3$), 3.81 (q, 1H, *J* = 8.00 Hz, -CH), 4.21–4.23 (m, 2H, -CH$_2$), 7.10–7.12 (m, 1H,

Ar-H), 7.26–7.30 (m, 2H, Ar-H), 7.52–7.60 (m, 4H, Ar-H), 7.65–7.68 (m, 2H, Ar-H), 7.73–7.78 (m, 3H, Ar-H), 8.6 (s, 1H, Ar-H), 10.07 (s, 1H, -NH). ^{13}C NMR (100 MHz, DMSO): δ 18.9, 42.1, 45.4, 118.5, 125.1, 126.7, 127.6, 128.6, 128.9, 129.0, 130.1, 132.1, 133.2, 136.8, 137.4, 138.8, 140.9, 143.1, 170.8, 173.4, 179.1, 196.3. MS(ESI): m/z = found 448.5 ([M + H]$^+$).

N-(4-isoselenocyanatobenzyl)-2-(6-methoxynaphthalen-2-yl)propenamide (**5c**)

Yield: 82%. White solid. Mp: 76–78 °C. ^{1}H NMR (400 MHz, DMSO): δ 1.46 (d, 3H, *J* = 8.00 Hz, -CH$_3$), 3.82 (q, 1H, *J* = 8.00 Hz, -CH), 3.87 (s, 3H, -OCH$_3$), 4.24–4.26 (m, 2H, -CH$_2$), 7.12–7.16 (m, 2H, Ar-H), 7.24–7.29 (m, 2H, Ar-H), 7.48–7.50 (m, 1H, Ar-H), 8.58–8.61 (m, 1H, Ar-H), 10.06 (s, 1H, -NH). ^{13}C NMR (100 MHz, DMSO): δ 19.0, 42.2, 45.6, 55.6, 106.2, 119.1, 125.1, 125.8, 126.7, 127.0, 128.1, 128.9, 129.6, 133.6, 137.0, 137.9, 138.7, 141.0, 157.5, 173.9. MS(ESI): m/z = found 424.8 ([M + H]$^+$).

N-(4-isoselenocyanatobenzyl)-2-((3-(trifluoromethyl)phenyl)amino)benzamide (**5d**)

Yield: 80%. White solid. Mp: 100–102 °C. ^{1}H NMR (400 MHz, CDCl$_3$): δ 4.60 (d, 2H, *J* = 8.00 Hz, -CH$_2$), 6.59–6.62 (m, 1H, Ar-H), 6.82–6.86 (m, 1H, Ar-H), 7.22–7.24 (m, 1H, Ar-H), 7.31–7.48 (m, 8H, Ar-H), 9.49 (s, 1H, Ar-H). ^{13}C NMR (100 MHz, CDCl$_3$): δ 43.2, 116.0, 116.4 (d, *J* = 4 Hz), 118.5, 118.7 (d, *J* = 4 Hz), 119.2, 123.1, 124.0 (q, *J* = 271 Hz), 126.5, 127.6, 128.8, 129.6, 129.9, 131.7 (q, *J* = 32 Hz), 132.8, 138.3, 142.2, 144.6, 169.3. MS (ESI): m/z = found 475.5 ([M + 1]$^+$).

2-(2-fluoro-[1,1′-biphenyl]-4-yl)-*N*-(4-isoselenocyanatobenzyl)propenamide (**5e**)

Yield: 82%. White solid. Mp: 88–90 °C. ^{1}H NMR (400 MHz, CDCl$_3$): δ 1.56 (d, 3H, *J* = 8.00 Hz, -CH$_3$), 3.62 (q, 1H, *J* = 8.00 Hz, -CH), 4.38–4.40 (m, 2H, -CH$_2$), 5.91–5.94 (m, 1H, Ar-H), 7.10–7.21 (m, 5H, Ar-H), 7.37–7.45 (m, 4H, Ar-H), 7.51–7.54 (m, 2H, Ar-H). ^{13}C NMR (100 MHz, CDCl$_3$): δ 18.5, 43.0, 46.6, 115.3 (d, *J* = 23 Hz), 123.6 (d, *J* = 4 Hz), 126.4, 127.9, 128.3 (d, *J* = 13Hz), 128.6 (d, *J* = 7 Hz), 128.8, 128.9 (d, *J* = 3 Hz), 129.4 (NCSe), 131.2 (d, *J* = 4 Hz), 135.2, 138.7, 142.4 (d, *J* = 7 Hz), 158.6, 161.1, 173.6. MS (ESI): m/z = found 438.7 ([M + 1]$^+$).

2-(1,8-diethyl-1,3,4,9-tetrahydropyrano[3,4-b]indol-1-yl)-*N*-(4-isoselenocyanatobenzyl)acetamide (**5f**)

Yield: 78%. White solid. Mp: 107–109 °C. ^{1}H NMR (400 MHz, CDCl$_3$): δ 0.87 (t, *J* = 4.00 Hz, 3H, -CH$_3$), 1.24 (t, *J* = 4.00 Hz, -CH$_3$), 1.85–1.93 (m, 2H, -CH), 2.08–2.14 (m, 1H, -CH), 2.58–2.81 (m, 4H, 2CH$_2$), 3.01 (s, 2H, -CH$_2$), 4.03–4.09 (m, 2H, -CH$_2$), 4.26 (s, 3H, -OCH$_3$), 6.80–6.82 (m, 2H, Ar-H), 7.02–7.03 (m, 1H, Ar-H), 7.09–7.13 (m, 1H, Ar-H), 7.25–7.29 (m, 2H, Ar-H), 9.62 (s, 1H, Ar-H). ^{13}C NMR (100 MHz, CDCl$_3$): δ 7.7, 14.1, 22.2, 24.1, 31.2, 42.5, 43.8, 60.4, 76.0, 107.4, 115.8, 119.8, 120.6, 126.1, 126.3, 127.0, 128.2, 128.3, 129.1, 134.8, 135.5, 138.5, 171.4. MS(ESI): m/z = found 482.1 ([M + 1]$^+$).

2-((2,3-dimethylphenyl)amino)-*N*-(4-isoselenocyanatobenzyl)benzamide (**5g**)

Yield: 72%. White solid. Mp: 91–93 °C. ^{1}H NMR (400 MHz, DMSO): δ 2.08 (s, 3H, -CH$_3$), 2.26 (s, 3H, -CH$_3$), 4.51–4.53 (m, 2H, -CH$_2$), 6.74–6.75 (m, 1H, Ar-H), 6.83–6.85 (m, 1H, Ar-H), 6.92–6.94 (m, 1H, Ar-H), 7.04–7.09 (m, 2H, Ar-H), 7.45–7.55 (m, 3H, Ar-H), 7.71–7.76 (m, 1H, Ar-H), 9.19 (s, 1H, -NH), 9.58 (s, 1H, -NH). ^{13}C NMR (100 MHz, DMSO): δ 14.0, 20.7, 42.4, 114.4, 116.8, 117.2, 119.6, 120.5, 125.7, 126.3, 126.8, 127.0, 128.3, 128.6, 128.9, 129.1, 130.0, 132.7, 138.2, 139.6, 142.2, 147.0, 169.7. MS(ESI): m/z = found 435.1 ([M + Na]$^+$).

N-(4-isoselenocyanatobenzyl)-2-(4-((2-oxocyclopentyl)methyl)phenyl)propenamide (**5h**)

Yield: 75%. White solid. Mp: 86–88 °C. ^{1}H NMR (400 MHz, DMSO): δ 1.36 (d, *J* = 8.00 Hz, 3H, -CH$_3$), 1.45–1.51 (m, 1H, -CH), 1.66–1.73 (m, 1H, -CH), 1.82–1.93 (m, 2H, -CH$_2$), 2.02–2.11 (m, 1H, -CH), 2.21–2.26 (m, 1H, -CH), 2.36–2.46 (m, 2H, -CH), 2.94–2.97 (m, 1H, -CH), 3.62 (q, *J* = 8.00 Hz, 1H, -CH), 4.46 (d, *J* = 8.00 Hz, 2H, -CH$_2$), 7.11–7.13(m, 2H, Ar-H), 7.21–7.26 (m, 4H, Ar-H), 7.40–7.42 (m, 2H, Ar-H), 8.52 (s, 1H, -NH). ^{13}C NMR

(100 MHz, DMSO): δ 18.9, 20.5, 29.2, 35.0, 38.1, 42.0, 45.3, 50.5, 125.1, 126.6, 127.7, 128.1, 128.8, 129.1, 136.9, 138.8, 140.2, 140.3, 141.1, 173.9, 174.0, 179.0. MS(ESI): m/z = found 440.5 ([M + Na]$^+$).

4.2.4. General Procedure for the Synthesis of Compounds 6a–6h

Compound **5** (**a**–**h**) (1.0 eq.) was dissolved in CH$_3$OH (20 mL) at room temperature, then the solvent was refluxed for 4.0 h. TLC showed the reaction was complete. The desire compound was purified by column chromatogragraphy on silica gel.

O-methyl (4-((2-(4-isobutylphenyl)propanamido)methyl)phenyl) carbamoselenoate (**6a**)

Yield: 60%. White solid. Mp: 117–118 °C. ^{1}H NMR (400 MHz, CDCl$_3$): δ 0.88 (d, *J* = 8.00 Hz, 6H, 2CH$_3$), 1.44 (d, 3H, *J* = 8.00 Hz, -CH$_3$), 1.83 (q, 1H, *J* = 8.00 Hz, -CH), 2.44 (d, 2H, *J* = 8.00 Hz, -CH$_2$), 3.64 (q, 1H, *J* = 8.00 Hz, -CH), 4.12 (s, 3H, -OCH$_3$), 4.23–4.34 (m, 2H, -CH$_2$), 7.07–7.12 (m, 4H, Ar-H), 7.18–7.24 (m, 4H, Ar-H), 7.51 (brs, 1H, -NH). ^{13}C NMR (100 MHz, CDCl$_3$): δ 17.3, 21.3, 30.1, 42.1, 44.6, 45.8, 60.7, 121.8, 126.8, 127.5, 128.9, 136.1, 136.6, 139.0, 140.2, 175.8, 191.8. MS(ESI): m/z = found 455.1 ([M + Na]$^+$).

O-methyl (4-((2-(3-benzoylphenyl)propanamido)methyl)phenyl)carbamoselenoate (**6b**)

Yield: 62%. White solid. Mp: 88–90 °C. ^{1}H NMR (400 MHz, CDCl$_3$): δ 1.48 (d, *J* = 8.00 Hz, 3H, -CH$_3$), 3.77 (q, *J* = 8.00 Hz, 1H, -CH), 4.12 (s, 3H, -OCH$_3$), 4.25–4.35 (m, 2H, -CH$_2$), 7.11–7.18 (m, 3H, Ar-H), 7.45–7.51 (m, 4H, Ar-H), 7.60–7.64 (m, 3H, Ar-H), 7.72–7.76 (m, 3H, Ar-H). ^{13}C NMR (100 MHz, CDCl$_3$): δ 17.4, 42.2, 45.9, 60.7, 121.8, 124.1, 127.7, 128.2, 128.3, 128.7, 129.7, 131.4, 132.5, 135.9, 136.6, 137.3, 137.7, 142.2, 174.9, 191.8, 197.1. MS (ESI): m/z = found 503.0 ([M + Na]$^+$).

O-methyl (4-((2-(6-methoxynaphthalen-2-yl)propanamido)methyl)phenyl) carbamoselenoate (**6c**)

Yield: 55%. White solid. Mp: 93–95 °C. ^{1}H NMR (400 MHz, CDCl$_3$): δ 1.52 (d, *J* = 8.00 Hz, 3H, -CH$_3$), 3.79 (q, *J* = 8.00 Hz, 1H, -CH), 3.87 (s, 3H, -OCH$_3$), 4.12 (s, 3H, -OCH$_3$), 4.26–4.30 (m, 2H, -CH$_2$), 7.08–7.17 (m, 5H, Ar-H), 7.40–7.43 (m, 1H, Ar-H), 7.65–7.71 (m, 3H, Ar-H). ^{13}C NMR (100 MHz, CDCl$_3$): δ 17.4, 42.2, 46.1, 54.4, 60.7, 105.2, 118.5, 121.7, 124.1, 125.4, 125.8, 126.8, 127.6, 128.8, 129.0, 133.8, 136.1, 136.7, 157.7, 175.7, 191.7. MS(ESI): m/z = found 479.1 ([M + Na]$^+$).

O-methyl (4-((2-((3-(trifluoromethyl)phenyl)amino)benzamido)methyl)phenyl) carbamoselenoate (**6d**)

Yield: 65%. White solid. Mp: 101–102 °C. ^{1}H NMR (400 MHz, CDCl$_3$): δ 4.12 (s, 3H, -OCH$_3$), 4.46–4.48 (m, 2H, -CH$_2$), 6.89–6.93 (m, 1H, Ar-H), 7.14–7.16 (m, 1H, Ar-H), 7.21–7.38 (m, 9H, Ar-H), 7.62–7.65 (m, 1H, Ar-H). ^{13}C NMR (100 MHz, CDCl$_3$): δ 42.5, 64.8, 114.4 (*J* = 4.0 Hz), 116.9, 117.2 (*J* = 4.0 Hz), 120.0, 121.3, 121.5, 121.9, 122.9, 125.6, 127.8, 128.6, 129.8, 131.2 (q, *J* = 32 Hz, -CF$_3$), 131.9, 136.29 (d, *J* = 58 Hz), 143.1 (d, *J* = 32 Hz). MS (ESI): m/z = found 530.1 ([M + Na]$^+$).

O-methyl (4-((2-(2-fluoro-[1,1'-biphenyl]-4-yl)propanamido)methyl)phenyl)carbamoselenoate (**6e**)

Yield: 60%. White solid. Mp: 72–74 °C. ^{1}H NMR (400 MHz, CDCl$_3$): δ 1.56 (d, 3H, *J* = 8.00 Hz, -CH$_3$), 3.62 (q, *J* = 8.00 Hz, 1H, -CH), 4.21 (s, 3H, -OCH$_3$), 4.35–4.40 (m, 2H, -CH$_2$), 5.91–5.97 (m, 1H, -NH), 7.10–7.18 (m, 6H, Ar-H), 7.37–7.53 (m, 6H, Ar-H), 9.22 (brs, 1H, -NH). ^{13}C NMR (100 MHz, CDCl$_3$): δ 18.8, 42.2, 45.1, 61.6, 115.3 (d, *J* = 23 Hz), 122.6, 124.3, 125.2, 126.7, 127.0, 127.7, 128.1 (d, *J* = 7 Hz), 128.9, 129.1, 129.2, 130.9 (d, *J* = 3 Hz), 135.5, 136.8 (d, *J* = 19 Hz), 140.9, 144.6, 158.1, 160.5, 173.2 (d, *J* = 16 Hz), 190.7. MS (ESI): m/z = found 493.0 ([M + Na]$^+$).

O-methyl (4-((2-(1,8-diethyl-1,3,4,9-tetrahydropyrano[3,4-b]indol-1-yl)acetamido)methyl)phenyl)carbamoselenoate (**6f**)

Yield: 62%. White solid. Mp: 83–85 °C. ^{1}H NMR (400 MHz, CDCl$_3$): δ 0.87 (t, *J* = 4.00 Hz, 3H, -CH$_3$), 1.24 (t, *J* = 4.00 Hz, -CH$_3$), 1.87–2.14 (m, 2H, -CH$_2$), 2.63–2.80 (m, 4H, 2CH$_2$), 3.03 (s, 2H, -CH$_2$), 4.03–4.07 (m, 2H, -CH$_2$), 4.26 (s, 3H, -OCH$_3$), 6.78–6.85 (m, 3H, Ar-H), 7.00–7.13 (m, 2H, Ar-H), 7.24–7.29 (m, 2H, Ar-H). ^{13}C NMR (100 MHz, CDCl$_3$): δ 8.3, 14.9, 22.4, 24.2, 31.1, 42.0, 44.3, 60.4, 61.7, 76.0, 107.4, 115.9, 119.2, 120.1, 122.5, 126.5, 127.0, 127.9, 128.7, 134.9, 137.0, 141.0, 169.9, 190.6. MS(ESI): m/z = found 536.1 ([M + Na]$^+$).

O-methyl (4-((2-((2,3-dimethylphenyl)amino)benzamido)methyl)phenyl) carbamoselenoate (**6g**)

Yield: 62%. White solid. Mp: 83–85 °C. ^{1}H NMR (400 MHz, CDCl$_3$): δ 2.13 (s, 3H, -CH$_3$), 2.28 (s, 3H, -CH$_3$), 4.15 (s, 3H, -OCH$_3$), 4.50 (s, 2H, -CH$_2$), 6.69–6.73 (m, 1H, Ar-H), 6.79–6.81 (m, 1H, Ar-H), 6.91–6.93 (m, 1H, Ar-H), 7.02–7.05 (m, 2H, Ar-H). 7.17–7.21 (m, 1H, Ar-H), 7.25–7.32 (m, 4H, Ar-H), 7.57–7.61 (m, 1H, Ar-H). ^{13}C NMR (100 MHz, CDCl$_3$): δ 12.6, 19.3, 42.3, 60.7, 114.3, 116.8, 117.3, 120.6, 121.9, 125.4, 125.6, 127.7, 128.1, 130.3, 131.9, 136.3, 136.6, 137.7, 139.5, 146.8, 170.5, 191.8. MS (ESI): m/z = found 490.1 ([M + Na]$^+$).

O-methyl (4-((2-(4-((2-oxocyclopentyl)methyl)phenyl)propanamido)methyl)phenyl) carbamoselenoate (**6h**)

Yield: 68%. White solid. Mp: 109–111 °C. ^{1}H NMR (400 MHz, CD$_3$OD): 1.34 (d, 3H, *J* = 8.00 Hz, -CH$_3$), 1.45–1.50 (m, 1H, -CH-), 1.67–1.72 (m, 1H, -CH-), 1.83–1.92 (m, 2H, -CH$_2$), 2.02–2.11(m, 1H, -CH-), 2.21–2.26 (m, 1H, -CH-), 2.36–2.44 (m, 2H, -CH$_2$), 2.94–2.97 (m, 1H, -CH-), 3.62–3.63 (m, 1H, -CH-), 4.09 (m, 3H, -OCH$_3$), 4.18 (s, 2H, -CH$_2$), 7.11–7.13 (m, 4H, Ar-H), 7.23–7.27 (m, 4H, Ar-H), 8.44 (s, 1H, -NH), 11.7 (s. 1H, -NH). ^{13}C NMR (100 MHz, CD$_3$OD): 18.9, 20.5, 29.2, 35.0, 38.1, 42.1, 45.2, 50.5, 61.6. 122.6, 124.7, 127.7, 128.0, 129.0, 136.7, 137.1, 138.7, 140.3, 173.9, 190.7. MS (ESI): m/z = found 495.0 ([M + H]$^+$).

4.3. Cell Lines and Growth Conditions

Exponentially growing cells were harvested and plated on 96-well plates at a concentration of 1 × 104 cells/well. After 24 h incubation at 37 °C under a humidified 5% CO$_2$ to allow cell attachment, the cells in the wells were treated with target compounds at various concentrations for 48 h. The concentration of DMSO was always kept below 1.25%, which was found to be non-toxic to the cells. Three hours prior to experiment termination, MTT solution (20 μL of 5.0 mg/mL solution) was added to each well and incubated at 37 °C. At the termination timepoint, the medium/MTT mixtures were removed, and the formazan crystals formed by the mitochondrial dehydrogenase activity of vital cells were dissolved in 100 μL of DMSO per well. The optical densities were measured at 570 nm using a 96-well multiscanner (Dynex Technologies, MRX Revelation; Chantilly, VA, USA).

4.4. Detection of Bcl-2, IL-2 and Caspase-3 Molecular Biomarkers in MCF-7 Cells

Bcl-2, IL-2 and caspase-3 cells were evaluated in MCF-7 cells treated with the corresponding target compounds and incubated for 48 h and compared with their levels in control, untreated MCF-7 cell line. The cells were harvested by trypsinization and lysed by lysate buffer (Beyotime Biotech, Nanjing, China). Protein levels of Bcl-2, IL-2 and caspase-3 were measured using enzyme-linked immunosorbent assay (ELISA) by multifunctional enzyme marker (Molecular Devices i3, San Jose, CA, USA) at a wavelength of 570 nm.

4.5. DPPH Free Radical Scavenging Activity

DPPH free radical scavenging activity of corresponding compounds was measured according to the previously reported method with little optimization. In brief, 20 mL of test samples at different concentrations were mixed with 180 mL of or DPPH solution for 30 min in the dark. Then, the change in absorbance at 517 nm for DPPH was measured on

a microplate reader. Ascorbic acid (vitamin C) and ebselen were used as a positive control; DMSO was used as a negative control.

4.6. Bleomycin-Dependent DNA Damage

The reaction mixture contained DNA (0.5 mg/mL), bleomycin sulfate (0.05 mg/mL), $MgCl_2$ (5 mM), $FeCl_3$ (50 mM), and tested compound in a conc. of 0.1 mg/mL. L-ascorbic acid was used as positive control. The mixture was incubated at 37 °C for 1 h. The reaction was terminated by addition of 0.05 mL EDTA (0.1 M). The color was developed by adding 0.5 mL TBA (1% *w/v*) and 0.5 mL HCl (25% *v/v*), followed by heating at 80 °C for 30 min. After cooling in ice water, the extent of DNA damage was measured by the increase in absorbance at 532 nm.

4.7. Molecular Modeling

4.7.1. Protein and Ligand Preparation

The mammalian TrxR1 protein (PDB ID: 1H6V) used for docking was obtained from Protein Data Bank. The original structure was prepared using Protein Preparation Wizard in Maestro 11.5 (Schrödinger Release 2018-1: Maestro, Schrödinger, LLC, New York, NY, USA, 2018), with all but one subunit (E) discarded, bond orders assigned, hydrogens added, ionization and tautomerization state adjusted, hydrogen bond assignment optimized, waters removed, and structure minimized.

The LigPrep utility in Maestro 11.5 was used to perform ligand preparation, applying an OPLS3 force field. The generation of tautomers and possible ionization states was mediated by Epik utility. All stereoisomers were considered to be generated, followed by minimization of the resulting 3D conformations. There was no filtration process during preparation.

4.7.2. Ligand Docking

The docking task was carried out in Discovery Studio 2018 (Dassault Systèmes BIOVIA, Discovery Studio 2018, San Diego: Dassault Systèmes, 2018). The prepared TrxR1 protein was typed in CHARMm forcefield and the docking site was defined as a sphere with center coordinates X: 27.757, Y: 6.510, Z: 33.698 and a radius of 15 Å. Using Flexible Docking protocol, the residue sidechains within the site sphere were allowed to move. Ten protein conformations were created, with a maximum alteration of 8 residues. The FAST method was adopted; up to 25 conformations per ligand were generated with an energy threshold of 20 kcal. With all other parameters as default, ligands were preliminarily docked into each protein structure. After the removal of similar poses by clustering, the remaining complexes were refined and minimized, leading to a total of 133 final poses.

4.7.3. Result Analysis

The resulting 133 poses were clustered by ligand (53 for 3 h, 40 each for 2 h and 3 h) and visualized in Maestro 11.5. For each of the poses, the distance between the compound's selenium atom and the sulfur atom of either Cys497 or Cys498 was calculated as a measurement of covalent bonding probability. Any complex with less than 5 Å of the distance above was counted potentially reactive. For each ligand, average –CDocker energy and average selenium–sulfur distance were calculated; the latter was –CDocker energy weighted.

Institutional Review Board Statement: Not applicable.

Informed Consent Statement: Not applicable.

Data Availability Statement: Data are available from the corresponding authors upon reasonable request. ^{1}H, ^{13}C NMR and MS spectra of compounds are available from the Supplementary Materials.

Conflicts of Interest: The authors declare no conflict of interest.

Statistical Analysis

MTT data were given as mean $\pm$ SD of three independent experiments, graphs and curve fitting were using origin Version 8.0 (OriginLab Corporation, Northampton, MA, USA). *p* value less than 0.05 was considered statistically significant.

References

1. Maniar, K.H.; Jones, I.A.; Gopalakrishna, R.; Vangsness, C.T. Lowering side effects of NSAID usage in osteoarthritis: Recent attempts at minimizing dosage. *Expert Opin. Pharmacother.* **2018**, *19*, 93–102. [CrossRef] [PubMed]
2. Benbow, T.; Campbell, J. Microemulsions as transdermal drug delivery systems for nonsteroidal anti-inflammatory drugs (NSAIDs): A literature review. *Drug Dev. Ind. Pharm.* **2019**, *45*, 1849–1855. [CrossRef] [PubMed]
3. Waddell, W.R.; Loughry, R.W. Sulindac for polyposis of the colon. *J. Surg. Oncol.* **1983**, *24*, 83–87. [CrossRef] [PubMed]
4. Palayoor, S.T.; Tofilon, P.J.; Coleman, C.N. Ibuprofen-mediated reduction of hy- poxia-inducible factors HIF-1alpha and HIF-2alpha in prostate cancer cells. *Clin. Cancer Res.* **2003**, *9*, 3150–3157.
5. Takiuchi, T.; Blake, E.A.; Matsuo, K.; Sood, A.K.; Brasky, T.M. Aspirin use and endometrial cancer risk and survival. *Gynecol. Oncol.* **2018**, *148*, 222–232. [CrossRef]
6. Wong, R.S.Y. Role of nonsteroidal anti-inflammatory drugs (NSAIDs) in cancer. prevention and cancer promotion. *Adv. Pharmacol. Sci.* **2019**, *2019*, 3418975. [CrossRef]
7. Wrobel, J.K.; Power, R.; Toborek, M. Biological activity of selenium: Revisited. *IUBMB Life* **2016**, *68*, 97–105. [CrossRef]
8. Hosnedlova, B.; Kepinska, M.; Skalickova, S.; Fernandez, C.; Ruttkay-Nedecky, B.; Malevu, T.D.; Sochor, J.; Baron, M.; Melcova, M.; Zidkova, J.; et al. A summary of new findings on the biological effects of selenium in selected animal species-a critical review. *Int. J. Mol. Sci.* **2017**, *18*, 2209. [CrossRef]
9. Vinceti, M.; Filippini, T.; Cilloni, S.; Crespi, C.M. The Epidemiology of Selenium and Human Cancer. *Adv. Cancer Res.* **2017**, *136*, 1–48.
10. Vinceti, M.; Filippini, T.; del Giovane, C.; Dennert, G.; Zwahlen, M.; Brinkman, M.; Zeegers, M.P.; Horneber, M.; D'Amico, R.; Crespi, C.M. Selenium for preventing cancer. *Cochrane Database Syst. Rev.* **2018**, *1*, CD005195. [CrossRef]
11. Murdolo, G.; Bartolini, D.; Tortoioli, C.; Piroddi, M.; Torquato, P.; Galli, F. Selenium and Cancer Stem Cells. *Adv. Cancer Res.* **2017**, *136*, 235–257. [PubMed]
12. El-Bayoumy, K. Overview: The late Larry C. Clark showed the bright side of the moon element (selenium) in a clinical cancer prevention trial. *Nutr. Cancer* **2001**, *40*, 4–5. [CrossRef] [PubMed]
13. Guo, P.; Wang, Q.; Liu, J.; Liu, L.; Zhao, P.; Cao, Y.; Liu, Y.; Qi, C. Preparation of two organoselenium compounds and their induction of apoptosis to SMMC-7221 cells. *Biol. Trace Elem. Res.* **2013**, *154*, 304–311. [CrossRef]
14. Desai, D.; Salli, U.; Vrana, K.E.; Amin, S. SelSA, selenium analogs of SAHA as potent histone deacetylase inhibitors. *Bioorg. Med. Chem. Lett.* **2010**, *20*, 2044–2047. [CrossRef] [PubMed]
15. Pinto, J.T.; Sinha, R.; Papp, K.; Facompre, N.D.; Desai, D.; El-Bayoumy, K. Differential effects of naturally occurring and synthetic organoselenium compounds on biomarkers in androgen responsive and androgen independent human prostate carcinoma cells. *Int. J. Cancer* **2007**, *120*, 1410–1417. [CrossRef]
16. Singh, U.; Null, K.; Sinha, R. In vitro growth inhibition ofmouse mammary epithelial tumor cells by methylseleninic acid: Involvement of protein kinases. *Mol. Nutr. Food Res.* **2008**, *52*, 1281–1288. [CrossRef]
17. Sharma, A.K.; Sharma, A.; Desai, D.; Madhunapantula, S.V.; Huh, S.J.; Robertson, G.P.; Amin, S. Synthesis and antiproliferative activity comparison of phenylalkyl isoselenocyanates with corresponding naturally occurring and synthetic isothiocyanates. *J. Med. Chem.* **2008**, *51*, 7820–7826. [CrossRef]
18. Moreno, E.; Plano, D.; Lamberto, I.; Font, M.; Encio, I.; Palop, J.A.; Sanmartin, C. Sulfur and selenium derivatives of quinazoline and pyrido [2,3-d]pyrimidine: Synthesis and study of their potential cytotoxic activity in vitro. *Eur. J. Med. Chem.* **2012**, *47*, 283–298. [CrossRef]
19. Desai, D.; Sinha, I.; Null, K.; Wolter, W.; Suckow, M.A.; King, T.; Amin, S.; Sinha, R. Synthesis and antitumor properties of selenocoxib-1 against rat prostate adenocarcinoma cells. *Int. J. Cancer* **2010**, *127*, 230–238. [CrossRef]

20. Plano, D.; Karelia, D.N.; Pandey, M.K.; Spallholz, J.E.; Amin, S.; Sharma, A.K. Design, synthesis, and biological evaluation of novel selenium (Se-NSAID) molecules as anticancer agents. *J. Med. Chem.* **2016**, *59*, 1946–1959. [CrossRef]

21. Liu, L.; Li, S.; Li, X.; Zhong, M.; Lu, Y.; Yang, J.; Zhang, Y.; He, X. Synthesis of NSAIDs-Se derivatives as potent anticancer agents. *Med. Chem. Res.* **2018**, *27*, 2071–2078. [CrossRef]

22. Nie, Y.; Zhong, M.; Li, S.; Li, X.; Zhang, Y.; Zhang, Y.; He, X. Synthesis and potential. anticancer activity of some novel selenocyanates and diselenides. *Chem. Biodivers.* **2020**, *17*, e1900603. [CrossRef]

23. He, X.; Zhong, M.; Li, S.; Li, X.; Li, Y.; Li, Z.; Gao, Y.; Ding, F.; Wen, D.; Lei, Y.; et al. Synthesis and biological evaluation of organoselenium (NSAIDs-SeCN and SeCF3) derivatives as potential anticancer agents. *Eur. J. Med. Chem.* **2020**, *208*, 112864. [CrossRef] [PubMed]

24. He, X.; Nie, Y.; Zhong, M.; Li, S.; Li, X.; Guo, Y.; Liu, Z.; Gao, Y.; Ding, F.; Wen, D.; et al. New organoselenides (NSAIDs-Se derivatives) as potential anticancer agents: Synthesis, biological evaluation and in silico calculations. *Eur. J. Med. Chem.* **2021**, *218*, 113384. [CrossRef]

25. Wittmann, C.; Chockley, P.; Singh, S.K.; Pase, L.; Lieschke, G.J.; Grabher, C. Hydrogen peroxide in inflammation: Messenger, guide, and assassin. *Adv. Hematol.* **2012**, *2012*, 541471. [CrossRef]

26. Jamier, V.; Ba, L.A.; Jacob, C. Selenium-and tellurium-containing multifunctional redox agents as biochemical redox modulators with selective cytotoxicity. *Chem. A Eur. J.* **2010**, *16*, 10920–10928. [CrossRef]

27. Pathania, D.; Sechi, M.; Palomba, M.; Sanna, V.; Berrettini, F.; Sias, A.; Taheri, L.; Neamati, N. Design and discovery of novel quinazolinedione-based redox modulators as therapies for pancreatic cancer. *Biochim. Biophys. Acta (BBA) Gen. Subj.* **2014**, *1840*, 332–343. [CrossRef] [PubMed]

28. Plano, D.; Baquedano, Y.; Ibáñez, E.; Jiménez, I.; Palop, J.A.; Spallholz, J.E.; Sanmartín, C. Antioxidant-prooxidant properties of a new organoselenium compound library. *Molecules* **2010**, *15*, 7292–7312. [CrossRef]

29. Lagunes, I.; Begines, P.; Silva, A.; Galán, A.R.; Puerta, A.; Fernandes, M.X.; Maya, I.; Fernández-Bolaños, J.G.; López, Ó.; Padrón, J.M. Selenocoumarins as new multitarget antiproliferative agents: Synthesis, biological evaluation and in silico calculations. *Eur. J. Med. Chem.* **2019**, *179*, 493–501. [CrossRef]

30. Meriane, D.; Genta-Jouve, G.; Kaabeche, M.; Michel, S.; Boutefnouchet, S. Rapid identification of antioxidant compounds of Genista saharae coss. & dur. By combination of DPPH scavenging assay and HPTLC-MS. *Molecules* **2014**, *19*, 4369–4379.

31. Uddin, R.; Saha, M.R.; Subhan, N.; Hossain, H.; Jahan, I.A.; Akter, R.; Alam, A. HPLC-analysis of polyphenolic compounds in gardenia jasminoides and determination of antioxidant activity by using free radical scavenging assays. *Adv. Pharm. Bull.* **2014**, *4*, 273–281. [PubMed]

32. Huang, D.; Qu, B.; Prior, R.L. The chemistry behind antioxidant capacity assays. *J. Agric. Food Chem.* **2005**, *53*, 1841–1856. [CrossRef] [PubMed]

33. Prior, R.L.; Wu, X.; Schaich, K. Standardized methods for the determination of. antioxidant capacity and phenolics in foods and dietary supplements. *J. Agric. Food Chem.* **2005**, *53*, 4290–4302. [CrossRef] [PubMed]

34. Tian, X.; Schaich, K.M. Effects of molecular structure on kinetics and dynamics of the trolox equivalent antioxidant capacity assay with ABTS(t*). *J. Agric. Food Chem.* **2013**, *61*, 5511–5519. [CrossRef]

35. Mira, A.; Gimenez, E.M.; Bolzan, A.D.; Bianchi, M.S.; Lopez-Larraza, D.M. Effect of thiol compounds on bleomycin-induced DNA and chromosome damage in human cells. *Arch. Environ. Occup. Health* **2013**, *68*, 107–116. [CrossRef]

36. Quispe-Tintaya, W.; Lee, M.; Dong, X.; Weiser, D.A.; Vijg, J.; Maslov, A.Y. Bleomycin-induced genome structural variations in normal, non-tumor cells. *Sci. Rep.* **2018**, *8*, 16523. [CrossRef]

37. Laffon, B.; Valdiglesias, V.; Pásaro, E.; Méndez, J. The Organic selenium compound selenomethionine modulates bleomycin-induced DNA damage and repair in human leukocytes. *Biol. Trace. Elem. Res.* **2010**, *133*, 12–19. [CrossRef]

38. Bermingham, E.N.; Hesketh, J.E.; Sinclair, B.R.; Koolaard, J.P.; Roy, N.C. Selenium-enriched foods are more effective at increasing glutathione peroxidase (GPx) activity compared with selenomethionine: A meta-analysis. *Nutrients* **2014**, *6*, 4002–4031. [CrossRef]

39. Nogueira, C.W.; Rocha, J.B.T. Toxicology and pharmacology of selenium: Emphasis on synthetic organoselenium compounds. *Arch. Toxicol.* **2011**, *85*, 1313–1359. [CrossRef]

40. Hodage, A.S.; Phadnis, P.P.; Wadawale, A.; Priyadarsini, K.I.; Jain, V.K. Synthesis, characterization and structures of 2-(3,5-dimethylpyrazol-1-yl)ethylseleno derivatives and their probable glutathione peroxidase (GPx) like activity. *Org. Biomol. Chem.* **2011**, *9*, 2992–2998. [CrossRef]

41. Nascimento, V.; Alberto, E.E.; Tondo, D.W.; Dambrowski, D.; Detty, M.R.; Nome, F.; Braga, A.L. GPx-Like activity of selenides and selenoxides: Experimental evidence for the involvement of hydroxy perhydroxy selenane as the active species. *J. Am. Chem. Soc.* **2012**, *134*, 138–141. [CrossRef] [PubMed]

42. Gromer, S.; Wessjohann, L.A.; Eubel, J.; Brandt, W. Mutational studies confirm the catalytic triad in the human selenoenzyme thioredoxin reductase predicted by molecular modeling. *Chem. Biochem.* **2006**, *7*, 1649–1652. [CrossRef] [PubMed]

43. Brandt, W.; Wessjohann, L.A. The functional role of selenocysteine (Sec) in the catalysis mechanism of large thioredoxin reductases: Proposition of a swapping catalytic triad including a Sec-His-Glu state. *Chembiochem* **2005**, *6*, 386–394. [CrossRef] [PubMed]

44. Sandalova, T.; Zhong, L.; Lindqvist, Y.; Holmgren, A.; Schneider, G. Three dimensional structure of a mammalian thioredoxin reductase: Implications for mechanism and evolution of a selenocysteine-dependent enzyme. *Proc. Natl. Acad. Sci. USA* **2001**, *98*, 9533–9538. [CrossRef]

45. Shaaban, S.; Negm, A.; Ashmawy, A.M.; Ahmed, D.M.; Wessjohann, L.A. Combinatorial synthesis, in silico, molecular and biochemical studies of tetrazole-derived organic selenides with increased selectivity against hepatocellular carcinoma. *Eur. J. Med. Chem.* **2016**, *122*, 55–71. [CrossRef] [PubMed]